DØnote 4881

A Study of Mixing in the $B_s^0 - \bar{B}_s^0$ System Using the $B_s^0 \to D_s^- \mu^+ X,\ D_s^- \to \phi\pi^-$ Decay Mode And Opposite-Side Flavor Tagging

The DØ Collaboration

(Dated: July 18, 2005)

A search for $B_s^0 - \bar{B}_s^0$ oscillations was performed with a large sample of semileptonic B_s^0 decays corresponding to approximately 610 pb^{-1} of integrated luminosity accumulated with the DØ Detector in Run II at Fermilab (Tevatron). The flavor of the final state of the B_s^0 meson was determined using the muon charge from the partially reconstructed decay $B_s^0 \to \mu^+ D_s^- X$, $D_s^- \to \phi\pi^-$, $\phi \to K^+K^-$. An opposite-side tagging method was used for the initial-state flavor determination. A 95% confidence level limit on the oscillation frequency $\Delta m_s > 6.9$ ps^{-1} and sensitivity 7.8 ps^{-1} were obtained. A combination with the $B_s^0 \to \mu^+ D_s^- X$, $D_s^- \to K^{*0}K^-$ decay mode improves the result for the limit to $\Delta m_s > 7.3$ ps^{-1} and sensitivity to 9.5 ps^{-1}.

Preliminary Results for Summer 2005 Conferences

I. INTRODUCTION

One of the most interesting topics in B physics is B_s^0 mixing and the measurement of Δm_s. Combining Δm_s and Δm_d would allow a reduction in the theoretical uncertainty on V_{td}, and provide a critical test of the CKM formalism of the Standard Model. Currently the Tevatron is the only place in the world where B_s^0 mixing can be measured. No measurement of B_s^0 mixing exists, and the current limit is $\Delta m_s > 14.4$ ps^{-1} at the 95% CL [1]. Global fits to the unitarity triangle give $\Delta m_s = 18.3 \pm 1.7$ ps^{-1} which is in the range (15.6 – 22.2) ps^{-1} at the 95% CL if the current experimental limits on Δm_s are taken into account. Otherwise, global fits give $\Delta m_s = 20.6 \pm 3.5$ ps^{-1} which is in the range (14.2 – 28.1) ps^{-1} at the 95% CL [2].

II. DETECTOR DESCRIPTION

The following main elements of the DØ detector are essential for this analysis:

- The magnetic central-tracking system, which consists of a silicon microstrip tracker (SMT) and a central fiber tracker (CFT), both located within a 2 T superconducting solenoidal magnet;
- The muon system located beyond the calorimeter.

The SMT has $\approx 800,000$ individual strips, with typical pitch of $50 - 80$ μm, and a design optimized for tracking and vertexing capability at $|\eta| < 3$, where $\eta = -\ln(\tan(\theta/2))$ and θ is a polar angle. The CFT has eight thin coaxial barrels, each supporting two doublets of overlapping scintillating fibers of 0.835 mm diameter, one doublet being parallel to the collision axis, and the other alternating by $\pm 3°$ relative to the axis.

The muon system consists of a layer of tracking detectors and scintillation trigger counters before 1.8 T toroids, followed by two additional layers after the toroids. Tracking at $|\eta| < 1$ relies on 10 cm wide drift tubes, while 1 cm mini-drift tubes are used at $1 < |\eta| < 2$.

III. DATA SAMPLE

This analysis uses a $B \to \mu^+ D_s^- X$, $D_s^- \to \phi\pi^-$, $\phi \to K^+K^-$ data sample selected with an offline filter from all data taken from April 2002 to May 2005 with no trigger requirement. The selections for the offline filter are described below.

For this analysis muons were required to have $p_T > 2$ GeV/c and $p > 3$ GeV/c, to have hits both in the CFT and SMT and to have at least 2 measurements in the muon chambers.

All charged particles in the event were clustered into jets using the DURHAM clustering algorithm [3] with a p_T cut-off parameter set at 15 GeV/c [4]. The D_s^- candidate was constructed from three particles included in the same jet as the reconstructed muon. Two of these particles should give the ϕ meson mass after assigning them kaon masses (K_1 and K_2): $1.004 < M_{KK} < 1.034$ GeV. The third one must have a charge opposite to the muon charge. All three particles should have hits in the SMT and CFT. The transverse momentum was required to be $p_T > 0.7$ GeV/c for the kaons and $p_T > 0.5$ GeV/c for the pion. They should form a common D_s-vertex with $\chi^2_D < 16$ of the vertex fit. The vertexing algorithm is described in detail in [5]. For each particle, the transverse ϵ_T and longitudinal ϵ_L projections of the track impact parameter with respect to the primary vertex together with the corresponding errors ($\sigma(\epsilon_T)$, $\sigma(\epsilon_L)$) were computed. The combined significance $(\epsilon_T/\sigma(\epsilon_T))^2 + (\epsilon_L/\sigma(\epsilon_L))^2$ was required to be greater than 4 for the kaons. The distance d_T^D between the primary and D vertices in the transverse plane was required to exceed 4 standard deviations: $d_T^D/\sigma(d_T^D) > 4$. The angle α_T^D between the D_s^- momentum and the direction from the primary to D_s^- vertex in the transverse plane should satisfy the condition $\cos(\alpha_T^D) > 0.9$.

The tracks of the muon and D_s^- candidate were required to produce a common B-vertex with $\chi^2_B < 9$ of vertex fit. The transverse momentum of a B_s^0-hadron $p_T^{\mu D_s^-}$ was defined as the vector sum of transverse momenta of muon and D_s^-. The mass of the $(\mu^+ D_s^-)$ system should be within the limits: $2.6 < M(\mu^+ D_s^-) < 5.4$ GeV/c^2. The transverse decay length of a B_s^0-hadron d_T^B was defined as the distance in the transverse plane between the primary vertex and the vertex produced by the muon and D_s^-. If the distance d_T^B exceeded $4 \cdot \sigma(d_T^B)$, the angle α_T^B between the B momentum and the direction from the primary to B vertex in the transverse plane was required to satisfy the condition $\cos(\alpha_T^B) > 0.95$. The distance d_T^B was allowed to be greater than d_T^D, provided that the distance between the B and D vertices d_T^{BD} was less than $2 \cdot \sigma(d_T^{BD})$.

The final event samples were selected using a likelihood ratio method, described below.

A set of discriminating variables $x_1, ...x_n$ is constructed for a given event. The probability density functions $f^s(x_i)$ for the signal and $f^b(x_i)$ for the background are built for each variable x_i. The combined tagging variable y is defined as:

$$y = \prod_{i=1}^{n} y_i; \quad y_i = \frac{f_i^b(x_i)}{f_i^s(x_i)}. \tag{1}$$

Figure 1 shows the distributions of $-\log_{10} y$ for signal and background candidates. The variable x_i can be undefined for some events. In this case, the corresponding variable y_i is set to 1. The selection of the signal is obtained by applying the cut on $y < y_0$. For uncorrelated variables $x_1, ...x_n$, the selection using the combined variable y gives the best possible tagging performance, i.e., the maximal signal efficiency for a given background efficiency.

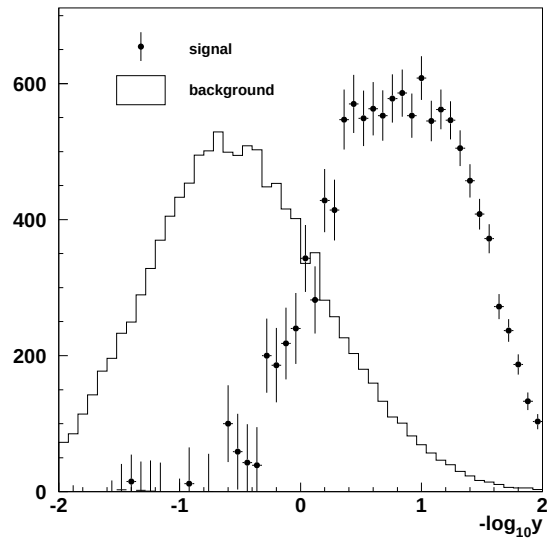

FIG. 1: Variable $-\log_{10} y$ for signal and background candidates.

The following discriminating variables were used:

- Helicity angle, defined as the angle between the D_s and K_1 momenta in the (K_1, K_2) center of mass system;
- Isolation, computed as $Iso = p^{tot}(\mu D_s)/(p^{tot}(\mu D_s) + \sum p_i^{tot})$. The sum $\sum p_i^{tot}$ was taken over all charged particles in the cone $\sqrt{(\Delta\phi)^2 + (\Delta\eta)^2} < 0.5$, where $\Delta\eta$ and $\Delta\phi$ are the pseudorapidity and the azimuthal angle with respect to the (μD_s) direction. The μ, K_1, K_2 and π were not included in the sum;
- $p_T(K_1 K_2)$;
- Invariant mass, $M(\mu D_s)$;
- χ^2 of the D_s vertex fit;
- $M(K_1 K_2)$.

The probability density functions were constructed using the real data events. For each channel, three bands B_1, B_2 and S were defined as:

$$\begin{aligned} B_1 &: 1.75 < M(D_s) < 1.79 \text{ GeV}/c^2; \\ B_2 &: 2.13 < M(D_s) < 2.17 \text{ GeV}/c^2; \\ S &: 1.92 < M(D_s) < 2.00 \text{ GeV}/c^2. \end{aligned}$$

The background probability density function for each variable was constructed using events from B_1 and B_2 bands. The signal probability density function was constructed by subtracting the background, obtained as a sum of distributions in B_1 and B_2 bands, from the distribution of events in band S. The final cut on the combined variable $\log_{10} y < 0.12$ was selected by requiring the maximal value of $S/\sqrt{S + B_1 + B_2}$.

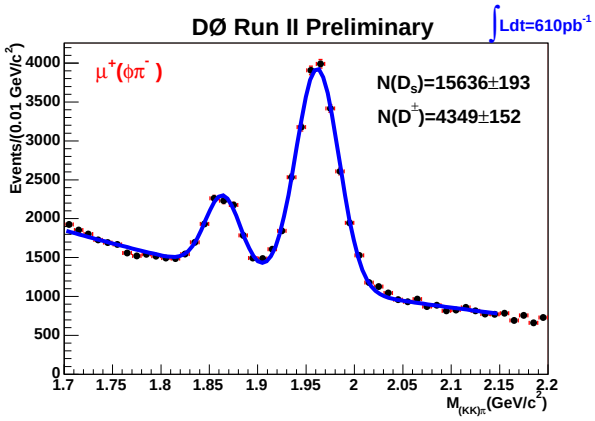

FIG. 2: $(KK)\pi$ invariant mass distribution for the untagged B_s sample. The peaks correspond to the $\mu D^{\pm}$ (left) and μD_s (right) candidates. The curve represent the fitting function to this mass spectrum (see Section V).

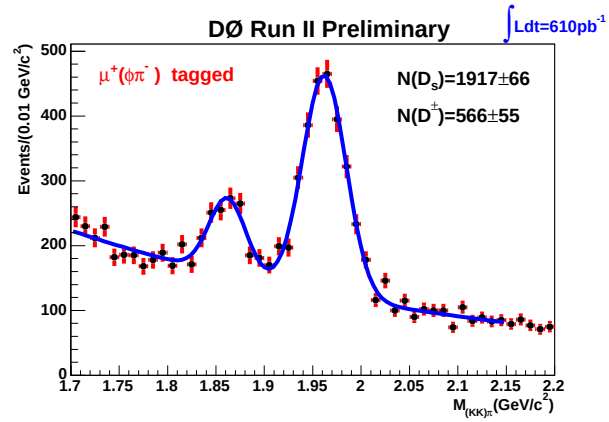

FIG. 3: $(KK)\pi$ invariant mass distribution for the tagged B_s sample. The peaks correspond to the $\mu D^{\pm}$ (left) and μD_s (right) candidates. The curve represent the fitting function to this mass spectrum (see Section V).

The total number of D_s^- candidates, passing this combined variable cut, in the mass peak is 15636 ± 193, while the number of $D^{\pm}$ candidates is 4349 ± 152 (Figure 2). There are 1917 ± 66 B_s^0 candidates which have an identified initial state flavor from the opposite-side tag (Figure 3).

IV. FLAVOR TAGGING

A necessary step in the B_s^0 oscillations analysis is the determination of the $B_s^0/\bar{B}_s^0$ initial and final state flavors. A presence of the muon in the B_s^0 semileptonic decay allows a determination of the final state flavor using relations $B_s^0 \to \mu^+ X$ and $\bar{B}_s^0 \to \mu^- X$.

The opposite-side tagging (OST) of the initial flavor of the B meson exploits the fact that in $b\bar{b}$ pair production there are always two particles containing b-quarks. A partial reconstruction of the B_s^0's partner gives an information with some certainty about the initial flavor of the B_s^0 meson. A subsample of all B candidates for which the partial reconstruction at the opposite-side is available is called below "*total tagged events*". The B_d and B_u mesons oscillate with low frequency or do not oscillate. Therefore, the B_d and B_u samples are used to determine the number of "*correctly tagged events*".

Purity, dilution and efficiency of the tagging are three useful parameters to describe the tagging performance. The purity of the tagging method is defined as $\eta_s = N_{correctly\ tagged\ events}/N_{total\ tagged\ events}$. The dilution is related to the purity with the simple formula $\mathcal{D} = 2\eta_s - 1$. Finally the tagging efficiency is defined as $\epsilon = N_{total\ tagged\ events}/N_{total\ events}$.

The tagging procedure, which exploits a presence of muon (electron) and/or secondary vertex at the opposite-side, is described in a separate note [6]. This note also describes a measurement of the B_d oscillation frequency and determination of the dilution for the B_d and B_u samples.

The B_d meson oscillation frequency was measured with the OST algorithm to be equal to:

$$\Delta m_d = 0.501 \pm 0.030\ (stat.) \pm 0.017\ (syst.)\ ps^{-1} \tag{2}$$

This result is in good agreement with the world average of $\Delta m_d = 0.502 \pm 0.007$ ps^{-1} [1]. One of the purposes of this measurement is to extract the dilutions for reconstructed B_d and B_u mesons: $\mathcal{D}_d = 0.414 \pm 0.023\ (stat.) \pm 0.006\ (syst.)$ and $\mathcal{D}_u = 0.368 \pm 0.016\ (stat.) \pm 0.002\ (syst.)$. The dilutions $\mathcal{D}_d$ and $\mathcal{D}_u$ are consistent; there is a 1.6σ difference between them. As an input to the B_s^0 mixing measurement procedure, we used the combined dilution $\mathcal{D}_s = 0.384 \pm 0.013\ (stat.) \pm 0.006\ (syst.)$ which was determine from the fit with the constraint $\mathcal{D}_s = \mathcal{D}_d = \mathcal{D}_u$. The lowest dilution $\mathcal{D}_u = 0.368$ was used for the systematic error.

V. MASS FITTING PROCEDURE

The number of B_s^0 candidates in the untagged sample is quite large. However, once the data is flavor tagged into mixed and unmixed samples and separated into bins of VPDL, the statistics in each bin are very much reduced. To

improve the fitting procedure, we first fit the full untagged sample and then fix the mass and width of the D_s from that sample when the flavor tagged samples are fit. For fitting the untagged sample, single Gaussians are used to describe the $D_s^{\pm} \to \phi\pi$ and $D^{\pm} \to \phi\pi$ decays, and the background is modeled by an exponential.

VI. EXPERIMENTAL OBSERVABLES A_i^{meas}

The proper lifetime of the B_s^0 meson, $ct_{B_s^0}$, for semileptonic decays can be written as

$$ct_{B_s^0} = x^M \cdot K, \quad \text{where} \quad x^M = (\mathbf{d_T^B} \cdot \mathbf{p_{xy}^{\mu D_s^-}})/(p_T^{\mu D_s^-})^2 \cdot M_B. \tag{3}$$

x^M is the *visible proper decay length* or VPDL. Semileptonic B decays necessarily have a neutrino present in the decay chain making a precise determination of the kinematics for the B meson impossible. In addition other neutrals or non-reconstructed charged particles can be present in the decay chain of the B meson. This leads to a bias towards smaller values of the B momentum calculated using the reconstructed particles. A common practice to correct this bias is to scale the measured momentum of the B by a K-factor, which takes into account the effects of neutrinos and other lost (or not used) particles. The K-factor was estimated from the MC simulation. For this analysis it was defined as:

$$K = p_T(\mu D_s^-)/p_T(B), \tag{4}$$

where p_T denotes the absolute value of transverse momentum.

Events were divided into 19 groups according to the measured VPDL. Intervals of VPDL for those groups are defined in Table I. The number of $\mu^+ D_s^-$ events with positive and negative tags, N_i^{osc} and $N_i^{non-osc}$, in each interval i were determined from a fit of the D_s^- peak in the mass $M(D_s^-)$ distribution.

The number of "non-oscillated" and "oscillated" events in each VPDL bin is given in Table I together with the corresponding errors derived from the fit.

TABLE I: Definition of 19 intervals in VPDL in the $\mu^+ D_s$ sample. For each interval this table lists the measured number of D_s for the opposite sign and same sign as the tag $N_i^{non-osc}, N_i^{osc}$, and their statistical errors $\sigma(N_i^{non-osc})$, $\sigma(N_i^{osc})$, all determined from the fits of corresponding mass M_{D_s} distributions. Also listed are the measured asymmetries A_i^{meas} and their errors $\sigma(A_i^{meas})$.

bin	VPDL range, cm	$N_i^{non-osc}$	$\sigma(N_i^{non-osc})$	N_i^{osc}	$\sigma(N_i^{osc})$	A_i^{meas}	$\sigma(A_i^{meas})$
1	[−0.01, 0.000]	35.50	8.89	34.71	8.81	0.011	0.178
2	[0.000, 0.005]	49.53	8.96	37.35	7.96	0.140	0.137
3	[0.005, 0.010]	27.99	8.16	53.37	9.06	-0.312	0.152
4	[0.010, 0.015]	44.34	9.34	45.32	9.06	-0.011	0.145
5	[0.015, 0.020]	41.85	9.32	55.52	9.66	-0.140	0.139
6	[0.020, 0.025]	57.25	9.97	51.89	9.04	0.049	0.123
7	[0.025, 0.030]	53.83	10.01	55.96	9.34	-0.019	0.125
8	[0.030, 0.035]	45.47	9.08	44.06	8.32	0.016	0.137
9	[0.035, 0.040]	30.91	7.96	53.03	9.33	-0.264	0.145
10	[0.040, 0.045]	44.00	8.65	43.89	8.30	0.001	0.136
11	[0.045, 0.050]	40.77	8.39	36.99	7.54	0.049	0.144
12	[0.050, 0.055]	51.77	9.09	28.64	6.83	0.288	0.136
13	[0.055, 0.060]	32.44	7.71	34.92	7.44	-0.037	0.159
14	[0.060, 0.080]	99.42	13.16	128.51	13.43	-0.128	0.083
15	[0.080, 0.100]	72.64	11.46	74.09	10.89	-0.010	0.108
16	[0.100, 0.120]	46.73	9.53	53.22	9.52	-0.065	0.135
17	[0.120, 0.150]	54.31	9.56	66.04	9.81	-0.097	0.114
18	[0.150, 0.180]	23.13	6.96	23.23	6.81	-0.002	0.210
19	[0.180, 0.210]	15.21	5.56	20.54	6.00	-0.149	0.229

The experimental observables, asymmetry A_i^{meas} in each VPDL bin, for this measurement were defined as:

$$A_i^{meas} = \frac{N_i^{non-osc} - N_i^{osc}}{N_i^{non-osc} + N_i^{osc}}; \tag{5}$$

where $N_i^{non-osc}$ is the number of events tagged as "non-oscillated" and N_i^{osc} is the number of events tagged as "oscillated". Figure 4 shows the asymmetry defined above as a function of the visible proper decay length. The wider VPDL bins have enough statistics to determine the asymmetry for the $\mu D^{\pm}$ sample (Figure 5). Contributions from the B^0 and $B^{\pm}$ decays to this sample were estimated at the level of 89% and 11% correspondingly. Assuming $\Delta m_s = 0.502$ ps^{-1} and $\mathcal{D} = \mathcal{D}_d = \mathcal{D}_u$ a fit to the asymmetry has been performed with the free $\mathcal{D}$ parameter. The output $\mathcal{D} = 0.460 \pm 0.101$ of the fit is in good agreement with the dilution $\mathcal{D}_s$ determined from the $\mu D^{*\pm}$ and μD^0 samples (see Section IV).

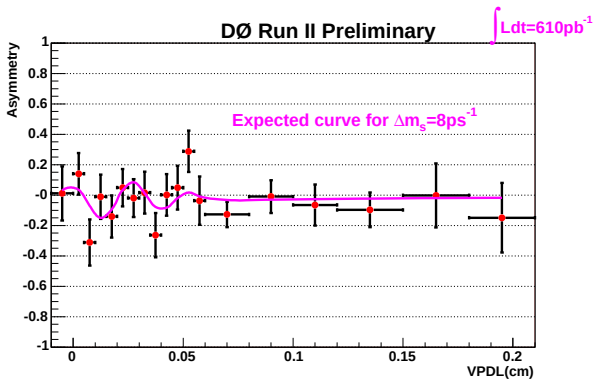

FIG. 4: Asymmetry in the μD_s sample as a function of the visible proper decay length (VPDL).

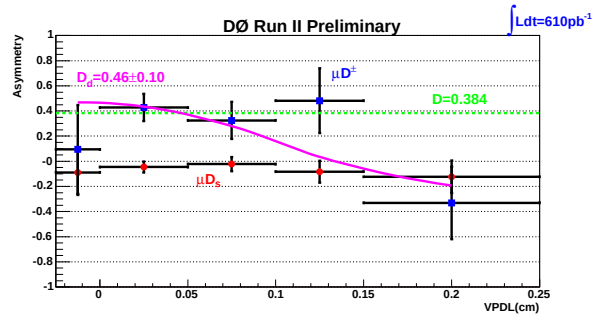

FIG. 5: Asymmetries in the μD_s and $\mu D^{\pm}$ samples as functions of the visible proper decay length (VPDL).

VII. FITTING PROCEDURE

The D_s^- sample is composed mostly of B_s^0 mesons with some contributions from B_u and B_d mesons. The small contributions from b-baryons are neglected. The different species of B mesons behave differently with respect to oscillations. Neutral B_d^0 and B_s mesons oscillate while charged B_u mesons do not, so we must take into account the different frequencies of oscillations during the fitting procedure.

For a given type of B-hadron (i.e. d, u, s), the distribution of the visible proper decay length, x, is given by:

$$n_s^{non-osc/osc}(x) = \frac{K}{c\tau_{B_s}} \exp\left(-\frac{Kx}{c\tau_{B_s}}\right) \cdot 0.5 \cdot [1 \pm (2\eta_s - 1)\cos(\Delta m_s \cdot Kx/c)]; \quad (6)$$

$$n_{D_sD_s}^{non-osc}(x) = n_{D_sD_s}^{osc}(x) = \frac{K}{c\tau_{B_s}} \exp\left(-\frac{Kx}{c\tau_{B_s}}\right) \cdot 0.5; \quad (7)$$

$$n_u^{non-osc}(x) = \frac{K}{c\tau_{B_u}} \exp\left(-\frac{Kx}{c\tau_{B_u}}\right) \cdot (1 - \eta_s); \quad (8)$$

$$n_u^{osc}(x) = \frac{K}{c\tau_{B_u}} \exp\left(-\frac{Kx}{c\tau_{B_u}}\right) \cdot \eta_s;$$

$$n_d^{non-osc/osc}(x) = \frac{K}{c\tau_{B_d}} \exp\left(-\frac{Kx}{c\tau_{B_d}}\right) \cdot 0.5 \cdot [1 \mp (2\eta_s - 1)\cos(\Delta m_d \cdot Kx/c)]; \quad (9)$$

where τ is the lifetime of B-hadrons taken from the PDG [1]. The $D_s^{\pm}$ charge has different correlations with the b-quark flavor in the B_u or B_d decays with respect to the B_s^0 semileptonic decays. The equations 8 and 9 take this into account.

The transition to the measured VPDL, x^M, is achieved by the integration over the K-factors and resolution functions:

$$N_{(d,u,s),\ j}^{osc,\ non-osc}(x^M) = \int dx\ Res_j(x - x^M, x) \cdot Eff_j(x) \cdot \theta(x) \int dK\ D_j(K) \cdot n_{(d,u,s),\ j}^{osc,\ non-osc}(x, K). \quad (10)$$

$Res_j(x - x^M, x)$ is the detector resolution of the VPDL and $Eff_j(x)$ is the reconstruction efficiency for a given decay channel j of this type of B meson. Both are determined from the MC simulation.

The expected number of oscillated/non-oscillated events in the i-th bin of VPDL is equal to

$$N_i^{e,osc/non-osc} = \int_i dx^M \left(\sum_{f=u,d,s} \sum_j (Br_j \cdot N_{f,\,j}^{osc/non-osc}(x^M)) \right). \tag{11}$$

The integration $\int_i dx^M$ is taken over a given interval i, the sum $\sum_j$ is taken over all decay channels $B \to \mu^+ \nu D^{*-} X$ and Br_j is the branching ratio of a given channel j.

Finally, the expected value A_i^e for interval i of the measured VPDL is given by Equation (5) with $N_i^{non-osc}$ and N_i^{osc} substituted by $N_i^{e,non-osc}$ and $N_i^{e,osc}$.

In order to set a limit on the value of Δm_s, we chose to use a technique called the amplitude fit method [8]. This technique requires us to modify Equation (6) to the following form

$$n_s^{non-osc/osc}(x) = \frac{K}{c\tau_{B_s}} \exp\left(-\frac{Kx}{c\tau_{B_s}}\right) \cdot 0.5 \cdot [1 \pm (2\eta_s - 1)\cos(\Delta m_s \cdot Kx/c) \cdot \mathcal{A}], \tag{12}$$

where $\mathcal{A}$ is now the only fit parameter.

The fitted values of $\mathcal{A}$ as a function of Δm_s were determined from the minimization of a $\chi^2(\mathcal{A})$ defined as:

$$\chi^2(\mathcal{A}) = \sum_i \frac{(A_i^{meas} - A_i^e(\mathcal{A}))^2}{\sigma^2(A_i^{meas})}. \tag{13}$$

The values of Δm_s were changed from 1 ps^{-1} to 20 ps^{-1} with a step size of 1 ps^{-1}. For each value of Δm_s the fitted value of $\mathcal{A}$ and its error were determined. To obtain a measurement of Δm_s one searches for a peak of $\mathcal{A} = 1$. If no peak is found then a limit can be set. The sensitivity of a measurement is determined by calculating the probability that $\mathcal{A} = 0$ could fluctuate to $\mathcal{A} = 1$. This occurs as 1.645σ (95% CL), where σ is the uncertainty associated with $\mathcal{A}$. The limit is determined by caclulating the probability that a fitted value of $\mathcal{A}$ could fluctuate to $\mathcal{A} = 1$. This occurs at $\mathcal{A} + 1.645\sigma < 1$.

VIII. INPUTS TO A_i^e

We have used the following measured parameters for B mesons from the PDG [1] as inputs for the fitting procedure: $c\tau_{B^+} = 501$ μm, $c\tau_{B^0} = 460$ μm, $c\tau_{B_s} = 438$ μm, and $\Delta m_d = 0.502$ ps^{-1}.

The latest PDG values were also used to determine the branching fractions of decays contributing to the D_s^- sample. We use the event generator EvtGen [9] since this code was developed specifically for the simulation of B decays. For those branching fractions not given in the PDG, we used the values provided by EvtGen, which are motivated by theoretical considerations. Taking into account the corresponding branching rates and reconstruction efficiencies, we determined the following contributions to our signal region from the various processes:

- $B_s^0 \to \mu^+ \nu D_s^-$: $(21.7 \pm 1.2)\%$;
- $B_s^0 \to \mu^+ \nu D_s^{-*} \to \mu^+ \nu D_s^- X$: $(60.7 \pm 3.2)\%$;
- $B_s^0 \to \mu^+ \nu D_{s0}^{*-} \to \mu^+ \nu D_s^- X$: $(1.4 \pm 0.5)\%$;
- $B_s^0 \to \mu^+ \nu D_{s1}^{'-} \to \mu^+ \nu D_s^- X$: $(3.1 \pm 0.5)\%$;
- $B_s^0 \to \tau^+ \nu D_s^- \to \mu^+ \nu D_s^- X$: $(1.3 \pm 0.5)\%$;
- $B_s^0 \to D_s^+ D_s^- X; D_s^- \to \mu\nu X$: $(2.9^{+1.1}_{-2.1})\%$;
- $B_s^0 \to D D_s^- X; D \to \mu\nu X$: $(0.9 \pm 0.5)\%$;
- $B^+ \to D D_s^- X; D \to \mu\nu X$: $(4.0 \pm 1.3)\%$;
- $B^0 \to D D_s^- X; D \to \mu\nu X$: $(4.1 \pm 1.4)\%$;

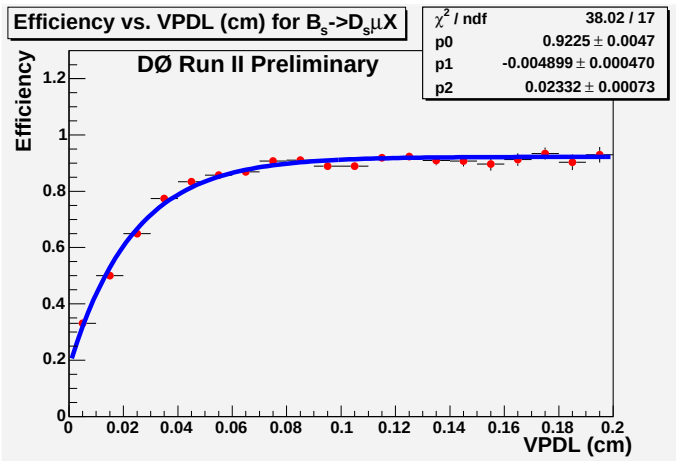

FIG. 6: Efficiency of the lifetime dependent cuts as a function of VPDL(cm) for $B_s \to \mu^+\nu D_s^- X$.

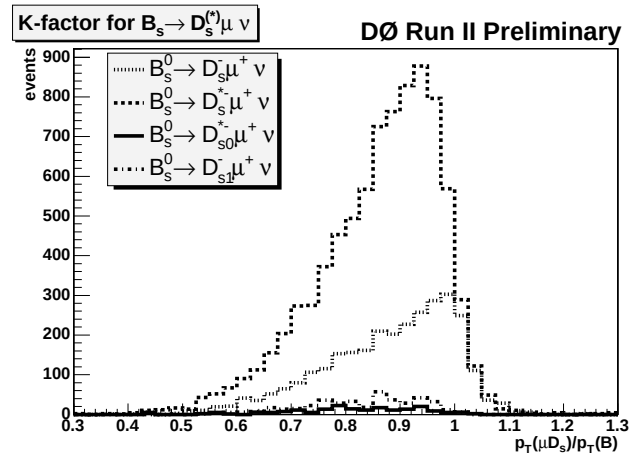

FIG. 7: K-factors for $B_s^0 \to \mu^+\nu D_s^-$; $B_s^0 \to \mu^+\nu D_s^{-*} \to \mu^+\nu D_s^-$; $B_s^0 \to \mu^+\nu D_{s0}^{*-} \to \mu^+\nu D_s^-$; $B_s^0 \to \mu^+\nu D_{s1}^{'-} \to \mu^+\nu D_s^-$ processes.

In the above numbers, the reconstruction efficiency does not include any lifetime cuts. We determined the efficiency of the lifetime selections for the sample as a function of VPDL as shown in Figure 6 for the decay $B_s \to \mu^+\nu D_s^- X$.

The background due to $c\bar{c}$ pairs originating from gluon splitting is an important contributor to the sample composition since they can produce the μD_s signature. For this to happen one c-quark must fragment to a D_s meson and the other c-quark must decay semileptonically. The OST used for this analysis requires either muon, electron or secondary vertex on the opposite side and therefore should suppress much of the $c\bar{c}$ contribution.

We estimate the $c\bar{c}$ contribution to the μD_s sample by using our estimate of this contribution to the μD^0 sample used for a previous D0 lifetime ratio analysis [7]. The $c\bar{c}$ contribution was determined to be $3.5 \pm 2.5\%$ after flavor tagging. The VPDL distribution for $c\bar{c}$ events was determined from MC.

In determining the K-factor, MC generator level information was used for the computation of p_T. Following the definition used in (4), the K-factors for all considered decays were calculated. Figure 7 shows the distributions of the K-factors for the semimuonic decays of the B_s. As expected, the K-factors for D_s^{-*}, D_{s0}^{*-} and $D_{s1}^{'-}$ have lower mean values because more decay products are lost. Since the K-factors in (4) were defined as the ratio of transverse momenta, they can exceed unity.

The decay length resolution for all samples was taken from the MC simulation and was parameterized by the sum of three Gaussians in the case of semileptonic B_s^0decays and by two Gaussians in all other cases.

One of the most important issues for B_s^0 mixing is the proper time resolution. We use MC simulation to determine the resolution. However, this assumes the uncertainties on the tracks are properly modeled in MC. We applied a tuning procedure similar to the one developed at DELPHI [10] and the overall scale factor was found to be equal to $SF = 1.142$. Figure 8 shows the VPDL resolution before and after the tuning procedure. The fit shows good agreement with the assumption that the scale factor is the same for all three Gaussians describing the resolution.

The VPDL resolutions have been found to depend on the VPDL. We describe this effect by using a variable scale factor SF for the VPDL resolution (Fig. 9). This dependence was implemented in the asymmetry fitting procedure.

IX. RESULTS

Figure 10 shows the dependence of the parameter $\mathcal{A}$ and its error on Δm_s. A 95% confidence level limit on the oscillation frequency $\Delta m_s > 7.0$ ps^{-1} and a sensitivity 8.1 ps^{-1} were obtained with statistical error only.

All studied contributions to the systematic uncertainty of the amplitude are listed in Tables II and III. For each Δm_s step the deviations of the $\Delta\mathcal{A}$ and $\Delta\sigma$ from the default values are given. One can see that the largest deviations come from the uncertainties in the $c\bar{c}$ contribution and the resolution. The resulting systematic errors were obtained using the following formula [8]:

$$\sigma_{\mathcal{A}}^{sys} = \Delta\mathcal{A} + (1 - \mathcal{A})\frac{\Delta\sigma_{\mathcal{A}}}{\sigma_{\mathcal{A}}} \tag{14}$$

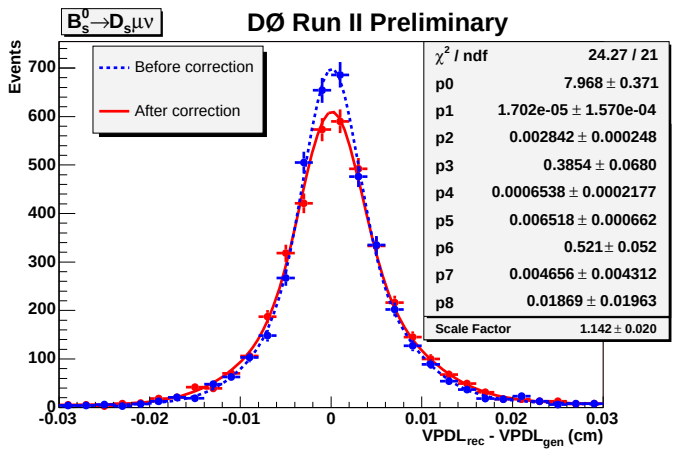

FIG. 8: Distribution of (reconstructed VPDL - generated VPDL) for decay $B_s \to \mu^+ \nu D_s^- X$ before and after the tuning procedure.

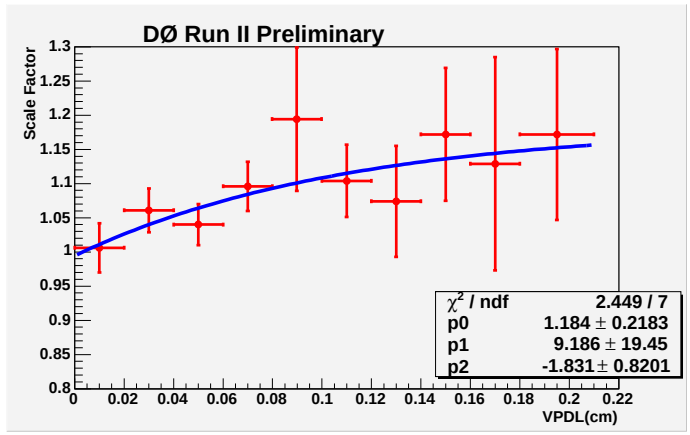

FIG. 9: The VPDL resolution scale factor as a function of VPDL.

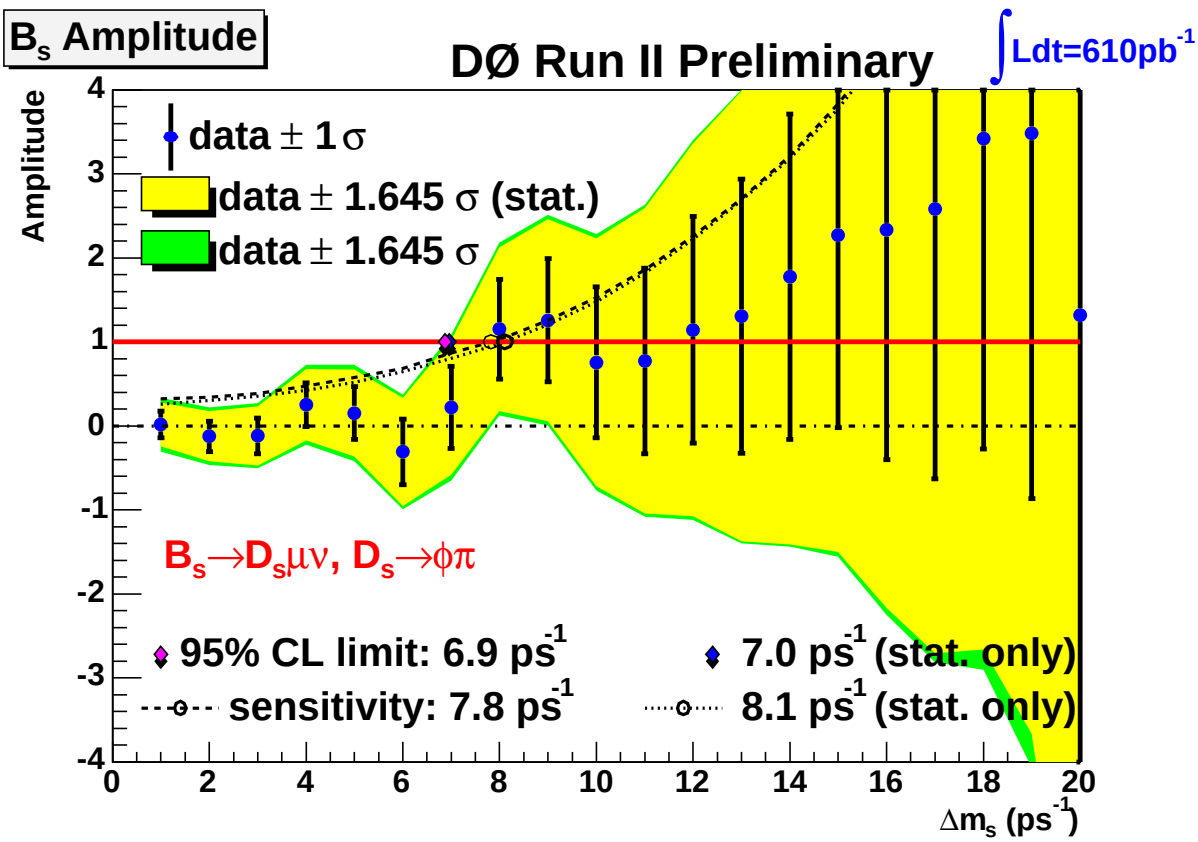

FIG. 10: B_s^0 oscillation amplitude with statistical (region "data±1.645σ (stat.)") and systematic (region "data±1.645σ") errors.

and summed in quadrature. The effect from the systematic errors is shown as a green region on Figure 10. Taking into account the systematic errors we obtain a 95% confidence level limit on the oscillation frequency $\Delta m_s > 6.9$ ps^{-1} and a sensitivity 7.8 ps^{-1}.

TABLE II: Systematic uncertainties on the amplitude. The shifts of both the measured amplitude, $\Delta\mathcal{A}$, and its statistical uncertainty, $\Delta\sigma$, are listed. Columns correspond to the different Δm_s steps.

Osc. frequency		1 ps^{-1}	2 ps^{-1}	3 ps^{-1}	4 ps^{-1}	5 ps^{-1}	6 ps^{-1}	7 ps^{-1}	8 ps^{-1}	9 ps^{-1}	10 ps^{-1}
Amplitude	$\mathcal{A}$	0.014	−0.125	−0.120	0.251	0.152	−0.310	0.222	1.150	1.257	0.755
Stat. uncertainty	σ^{stat}	0.158	0.182	0.214	0.258	0.313	0.391	0.489	0.593	0.731	0.898
$\eta_s = 0.684$	$\Delta\mathcal{A}$	+0.000	−0.004	−0.004	+0.012	+0.007	−0.013	+0.010	+0.050	+0.054	+0.033
	$\Delta\sigma$	+0.007	+0.008	+0.009	+0.011	+0.014	+0.017	+0.021	+0.026	+0.032	+0.039
$c\bar{c}$: 6%	$\Delta\mathcal{A}$	+0.003	−0.009	−0.010	+0.021	+0.004	−0.076	−0.032	+0.093	+0.098	−0.021
	$\Delta\sigma$	+0.009	+0.007	+0.008	+0.013	+0.018	+0.026	+0.037	+0.049	+0.067	+0.091
Br($D_s D_s$) = 4.7%	$\Delta\mathcal{A}$	+0.000	+0.003	+0.002	−0.005	−0.003	+0.006	−0.005	−0.024	−0.027	−0.018
	$\Delta\sigma$	−0.004	−0.004	−0.005	−0.006	−0.007	−0.008	−0.011	−0.013	−0.016	−0.019
Br($D_s \mu X$) = 5.5%	$\Delta\mathcal{A}$	+0.003	−0.020	−0.015	+0.001	−0.001	−0.016	+0.007	+0.049	+0.056	+0.033
	$\Delta\sigma$	+0.007	+0.008	+0.010	+0.012	+0.014	+0.018	+0.022	+0.027	+0.033	+0.040
$p_{T_\mu} > 4$ GeV/c	$\Delta\mathcal{A}$	+0.003	+0.015	+0.009	−0.000	+0.001	+0.006	−0.008	−0.030	−0.033	−0.026
	$\Delta\sigma$	−0.004	−0.005	−0.006	−0.007	−0.008	−0.011	−0.013	−0.016	−0.019	−0.024
$c\tau_{B_s^0} = 455\mu m$	$\Delta\mathcal{A}$	+0.002	−0.001	−0.001	+0.003	−0.002	−0.007	+0.004	+0.010	+0.002	−0.009
	$\Delta\sigma$	+0.000	+0.000	+0.000	+0.001	+0.001	+0.002	+0.002	+0.003	+0.004	+0.006
same eff. dependence	$\Delta\mathcal{A}$	+0.009	−0.001	−0.004	−0.001	−0.001	−0.008	−0.001	+0.012	+0.012	+0.003
for signal and bkg	$\Delta\sigma$	+0.001	+0.001	+0.002	+0.003	+0.003	+0.004	+0.005	+0.006	+0.008	+0.010
eff. slope varied	$\Delta\mathcal{A}$	+0.006	+0.001	−0.001	+0.001	−0.000	−0.007	−0.003	+0.006	+0.003	−0.011
by 1σ for signal	$\Delta\sigma$	+0.001	+0.001	+0.001	+0.002	+0.002	+0.003	+0.003	+0.004	+0.005	+0.006
Resolution $S.F. = 2$	$\Delta\mathcal{A}$	−0.006	+0.004	+0.007	+0.006	+0.000	+0.002	+0.002	−0.005	−0.007	−0.006
for background	$\Delta\sigma$	−0.000	+0.000	−0.000	−0.001	−0.001	−0.002	−0.003	−0.004	−0.005	−0.006
D_s mass changed to	$\Delta\mathcal{A}$	+0.002	−0.001	+0.000	−0.000	−0.002	−0.005	−0.003	+0.002	+0.001	+0.001
$M_s + 1\sigma$	$\Delta\sigma$	−0.000	−0.000	+0.000	−0.000	−0.000	+0.000	+0.000	+0.000	+0.000	−0.000
D_s width changed to	$\Delta\mathcal{A}$	+0.001	+0.002	−0.001	−0.001	+0.002	−0.000	−0.006	−0.010	−0.005	+0.008
$\sigma_s - 1\sigma$	$\Delta\sigma$	+0.000	+0.000	+0.000	+0.001	+0.001	+0.001	+0.001	+0.001	+0.001	+0.002
D^+ mass changed to	$\Delta\mathcal{A}$	+0.001	+0.000	−0.000	+0.001	+0.001	−0.000	−0.001	−0.002	−0.003	−0.005
$M_+ - 1\sigma$	$\Delta\sigma$	−0.000	−0.000	+0.000	−0.000	−0.000	+0.000	−0.000	−0.000	−0.000	−0.000
Slope for bkg.	$\Delta\mathcal{A}$	−0.000	−0.001	+0.001	−0.002	−0.004	−0.002	−0.003	−0.002	−0.003	−0.006
changed by 1σ	$\Delta\sigma$	−0.001	−0.002	−0.002	−0.002	−0.002	−0.003	−0.003	−0.004	−0.005	−0.006
Bkg. parametrized	$\Delta\mathcal{A}$	+0.004	+0.009	−0.005	+0.011	+0.017	−0.001	−0.014	−0.025	−0.007	+0.044
by straight line	$\Delta\sigma$	+0.008	+0.009	+0.010	+0.011	+0.012	+0.015	+0.018	+0.021	+0.026	+0.030
mass bin	$\Delta\mathcal{A}$	+0.010	−0.007	−0.000	+0.013	+0.047	+0.053	+0.024	+0.005	+0.011	−0.025
smaller by 50%	$\Delta\sigma$	−0.001	−0.001	−0.000	−0.002	−0.003	−0.002	−0.005	−0.007	−0.003	−0.002
$\Delta\Gamma/\Gamma = 0.2$	$\Delta\mathcal{A}$	−0.000	−0.001	+0.000	−0.000	−0.000	+0.001	+0.001	+0.001	+0.001	+0.002
	$\Delta\sigma$	+0.001	+0.001	+0.001	+0.001	+0.001	+0.001	+0.001	+0.001	+0.001	+0.001
Resolution $S.F. = 1.162$	$\Delta\mathcal{A}$	+0.001	−0.001	−0.004	+0.015	+0.024	−0.023	+0.009	+0.140	+0.188	+0.115
	$\Delta\sigma$	+0.001	+0.003	+0.006	+0.012	+0.020	+0.035	+0.055	+0.079	+0.112	+0.152
K-factor variation	$\Delta\mathcal{A}$	+0.003	+0.004	−0.009	−0.026	+0.043	+0.016	−0.134	−0.110	+0.064	+0.087
2%	$\Delta\sigma$	−0.001	−0.001	−0.001	−0.003	−0.008	−0.008	−0.011	−0.017	−0.022	−0.031
K-factor distribution	$\Delta\mathcal{A}$	+0.006	+0.001	−0.001	−0.001	+0.000	−0.004	−0.006	+0.001	+0.011	+0.011
smoothed	$\Delta\sigma$	+0.001	+0.001	+0.001	+0.001	+0.002	+0.002	+0.003	+0.004	+0.005	+0.006
K-factor from	$\Delta\mathcal{A}$	+0.000	−0.000	+0.000	−0.001	+0.001	+0.006	+0.001	−0.001	+0.014	+0.032
measured momenta	$\Delta\sigma$	+0.000	+0.000	+0.001	+0.001	+0.001	+0.002	+0.003	+0.004	+0.006	+0.007
$\mu D^\pm$ contribution	$\Delta\mathcal{A}$	−0.012	+0.005	+0.006	+0.011	+0.010	+0.004	+0.011	+0.019	+0.021	+0.020
1.6%	$\Delta\sigma$	+0.002	+0.003	+0.003	+0.004	+0.005	+0.006	+0.007	+0.009	+0.010	+0.013
Wide gaussion	$\Delta\mathcal{A}$	+0.026	+0.009	+0.016	−0.054	−0.058	+0.033	+0.049	+0.002	+0.066	+0.130
added in mass fit	$\Delta\sigma$	−0.001	−0.001	−0.000	−0.001	−0.004	−0.007	−0.010	−0.015	−0.016	−0.016
Total syst. error	σ^{sys}_{tot}	0.113	0.102	0.099	0.129	0.153	0.141	0.200	0.197	0.210	0.240
Total error	σ_{tot}	0.194	0.208	0.235	0.289	0.348	0.416	0.528	0.625	0.761	0.929

TABLE III: Continuation for Table II.

Osc. frequency		11 ps^{-1}	12 ps^{-1}	13 ps^{-1}	14 ps^{-1}	15 ps^{-1}	16 ps^{-1}	17 ps^{-1}	18 ps^{-1}	19 ps^{-1}	20 ps^{-1}
Amplitude	$\mathcal{A}$	0.773	1.141	1.304	1.774	2.272	2.334	2.581	3.417	3.482	1.316
Stat. uncertainty	σ^{stat}	1.106	1.349	1.629	1.936	2.295	2.737	3.214	3.696	4.346	5.418
$\eta_s = 0.684$	$\Delta\mathcal{A}$	+0.035	+0.052	+0.060	+0.082	+0.104	+0.108	+0.121	+0.158	+0.163	+0.075
	$\Delta\sigma$	+0.048	+0.059	+0.071	+0.084	+0.100	+0.119	+0.140	+0.161	+0.189	+0.236
$c\bar{c}$: 6%	$\Delta\mathcal{A}$	−0.039	+0.028	+0.047	+0.158	+0.299	+0.337	+0.497	+0.952	+1.266	+1.035
	$\Delta\sigma$	+0.123	+0.162	+0.213	+0.270	+0.341	+0.442	+0.556	+0.649	+0.783	+1.155
$\mathrm{Br}(D_s D_s) =$ 4.7%	$\Delta\mathcal{A}$	−0.018	−0.025	−0.030	−0.040	−0.051	−0.054	−0.061	−0.078	−0.081	−0.039
	$\Delta\sigma$	−0.024	−0.029	−0.035	−0.043	−0.049	−0.058	−0.068	−0.079	−0.094	−0.117
$\mathrm{Br}(D_s \mu X) =$ 5.5%	$\Delta\mathcal{A}$	+0.024	+0.029	+0.028	+0.041	+0.058	+0.052	+0.052	+0.076	+0.060	−0.084
	$\Delta\sigma$	+0.049	+0.060	+0.072	+0.089	+0.102	+0.121	+0.142	+0.165	+0.196	+0.247
${}^{p}T_{\mu} > 4$ GeV/c	$\Delta\mathcal{A}$	−0.025	−0.025	−0.027	−0.041	−0.049	−0.049	−0.062	−0.076	−0.051	+0.039
	$\Delta\sigma$	−0.029	−0.035	−0.042	−0.050	−0.059	−0.069	−0.080	−0.088	−0.112	−0.138
${}^{c\tau}B_s^0 = 455\mu m$	$\Delta\mathcal{A}$	−0.007	−0.002	−0.004	+0.003	+0.008	+0.004	+0.010	+0.033	+0.035	−0.025
	$\Delta\sigma$	+0.008	+0.011	+0.014	+0.017	+0.022	+0.028	+0.035	+0.041	+0.053	+0.078
same eff. dependence	$\Delta\mathcal{A}$	−0.001	−0.002	−0.008	−0.008	−0.008	−0.019	−0.029	−0.029	−0.046	−0.111
for signal and bkg	$\Delta\sigma$	+0.012	+0.015	+0.018	+0.020	+0.025	+0.030	+0.035	+0.041	+0.048	+0.060
eff. slope varied	$\Delta\mathcal{A}$	−0.022	−0.033	−0.051	−0.069	−0.093	−0.130	−0.172	−0.211	−0.272	−0.379
by 1σ for signal	$\Delta\sigma$	+0.007	+0.009	+0.010	+0.010	+0.011	+0.011	+0.011	+0.009	+0.006	+0.073
Resolution $S.F. = 2$	$\Delta\mathcal{A}$	−0.008	−0.008	−0.004	−0.004	−0.003	+0.005	+0.017	+0.029	+0.047	+0.061
for background	$\Delta\sigma$	−0.007	−0.008	−0.009	−0.011	−0.011	−0.010	−0.009	−0.008	−0.006	+0.008
D_s mass changed to	$\Delta\mathcal{A}$	+0.006	+0.004	−0.010	−0.016	−0.002	+0.013	+0.017	+0.020	+0.026	+0.034
$M_s + 1\sigma$	$\Delta\sigma$	+0.001	−0.000	−0.001	−0.001	−0.001	−0.001	−0.001	−0.001	−0.005	−0.005
D_s width changed to	$\Delta\mathcal{A}$	+0.016	+0.019	+0.023	+0.027	+0.032	+0.044	+0.048	+0.034	+0.021	+0.027
$\sigma_s - 1\sigma$	$\Delta\sigma$	+0.002	+0.002	+0.003	+0.003	−0.000	+0.004	+0.005	+0.005	+0.003	+0.006
D^+ mass changed to	$\Delta\mathcal{A}$	−0.008	−0.009	−0.010	−0.011	−0.013	−0.014	−0.017	−0.022	−0.028	−0.036
$M_+ - 1\sigma$	$\Delta\sigma$	−0.000	−0.001	−0.001	−0.001	−0.001	−0.001	−0.001	−0.001	−0.002	−0.002
Slope for bkg.	$\Delta\mathcal{A}$	−0.011	−0.013	−0.015	−0.020	−0.022	−0.023	−0.024	−0.023	−0.019	−0.008
changed by 1σ	$\Delta\sigma$	−0.008	−0.009	−0.011	−0.015	−0.022	−0.018	−0.021	−0.024	−0.029	−0.036
Bkg. parametrized	$\Delta\mathcal{A}$	+0.106	+0.125	+0.128	+0.161	+0.213	+0.268	+0.291	+0.272	+0.257	+0.269
by straight line	$\Delta\sigma$	+0.038	+0.046	+0.045	+0.065	+0.075	+0.088	+0.101	+0.115	+0.136	+0.199
mass bin	$\Delta\mathcal{A}$	−0.036	−0.028	−0.064	−0.069	+0.032	+0.060	−0.144	−0.429	−0.657	−0.840
smaller by 50%	$\Delta\sigma$	−0.004	−0.006	−0.001	+0.004	+0.003	−0.000	−0.009	−0.021	−0.036	−0.057
$\Delta\Gamma/\Gamma = 0.2$	$\Delta\mathcal{A}$	+0.002	+0.001	+0.002	+0.002	+0.001	+0.002	+0.003	+0.000	−0.000	−0.002
	$\Delta\sigma$	+0.001	+0.001	+0.001	+0.001	+0.001	+0.001	+0.001	+0.001	+0.002	+0.001
Resolution $S.F. = 1.162$	$\Delta\mathcal{A}$	+0.114	+0.170	+0.156	+0.202	+0.243	+0.126	−0.031	−0.059	−0.232	−0.541
	$\Delta\sigma$	+0.203	+0.212	+0.339	+0.427	+0.531	+0.657	+0.804	+0.965	+1.096	+1.147
K-factor variation	$\Delta\mathcal{A}$	−0.059	−0.061	−0.054	−0.168	−0.069	+0.039	−0.182	−0.317	+0.220	+1.269
2%	$\Delta\sigma$	−0.043	−0.053	−0.065	−0.077	−0.099	−0.131	−0.139	−0.150	−0.262	−0.421
K-factor distribution	$\Delta\mathcal{A}$	+0.003	−0.012	−0.015	−0.012	−0.003	−0.012	−0.015	−0.019	−0.023	−0.057
smoothed	$\Delta\sigma$	+0.008	+0.135	+0.013	+0.015	+0.018	+0.022	+0.025	+0.029	+0.034	+0.037
K-factor from	$\Delta\mathcal{A}$	+0.021	+0.009	+0.033	+0.036	+0.037	+0.056	+0.048	−0.024	−0.050	+0.022
measured momenta	$\Delta\sigma$	+0.009	+0.012	+0.014	+0.016	+0.018	+0.018	+0.018	+0.023	+0.027	+0.004
$\mu D^{\pm}$ contribution	$\Delta\mathcal{A}$	+0.027	+0.041	+0.053	+0.065	+0.076	+0.089	+0.104	+0.119	+0.136	+0.156
1.6%	$\Delta\sigma$	+0.015	+0.018	+0.022	+0.026	+0.030	+0.035	+0.040	+0.046	+0.053	+0.063
Wide gaussian	$\Delta\mathcal{A}$	−0.005	−0.145	−0.078	−0.104	−0.323	−0.383	−0.254	−0.245	−0.304	−0.235
added in mass fit	$\Delta\sigma$	−0.019	−0.020	−0.016	−0.017	−0.023	−0.040	−0.066	−0.082	−0.087	−0.094
Total syst. error	σ_{tot}^{sys}	0.225	0.261	0.213	0.263	0.401	0.532	0.650	1.058	1.468	2.002
Total error	σ_{tot}	1.129	1.374	1.643	1.953	2.330	2.788	3.279	3.844	4.587	5.776

X. COMBINATION WITH $D_s \to K^*K$ DECAY MODE

Another analysis [11] by the DØ collaboration used the $D_s \to K^*K$ decays to reconstruct the $B_s^0 \to \mu D_s X$ events for a B_s^0 oscillations measurement. A common procedure [12] was used for combination of the results in the $D_s \to K^*K$ and $D_s \to \phi\pi$ decay modes. The following contributions to the systematic error have been considered as correlated for these analyses:

- Uncertainty in purity ("$\eta_s = 0.684$" in Table II);
- Uncertainty in $c\bar{c}$ contamination ("$c\bar{c}:$ 6%" in Table II);
- Uncertainty in D_sD_s contribution ("Br$(D_sD_s) =$ 4.7%" in Table II);
- Uncertainty in branching ratio $B_s^0 \to \mu D_s X$ ("Br$(D_s\mu X) =$ 5.5%" in Table II);
- Uncertainty in B_s^0 lifetime ("$c\tau_{B_s^0} = 455\mu m$" in Table II);
- Non-zero $\Delta\Gamma_s/\Gamma_s$ ("$\Delta\Gamma/\Gamma = 0.2$" in Table II).

Figure 11 shows the dependence of the combined parameter $\mathcal{A}$ and its error on the Δm_s. A 95% confidence level limit on the oscillation frequency $\Delta m_s > 7.3$ ps^{-1} and sensitivity 9.5 ps^{-1} were obtained.

XI. CONCLUSIONS

Using a signal of 15.6k $B_s^0 \to \mu^+\nu D_s^- X$ ($D_s \to \phi\pi$, $\phi \to KK$) decays and an opposite-side flavor tagging algorithm, we performed a search for $B_s^0 - \bar{B}_s^0$ oscillations. We obtain a 95% confidence level limit on the oscillation frequency $\Delta m_s > 6.9$ ps^{-1} and a sensitivity of 7.8 ps^{-1}. A combination with the $B_s^0 \to \mu^+ D_s^- X$, $D_s^- \to K^{*0}K^-$ decay mode [11] improves the result for the limit to $\Delta m_s > 7.3$ ps^{-1} and sensitivity to 9.5 ps^{-1}.

Acknowledgments

We thank the staffs at Fermilab and collaborating institutions, and acknowledge support from the DOE and NSF (USA); CEA and CNRS/IN2P3 (France); FASI, Rosatom and RFBR (Russia); CAPES, CNPq, FAPERJ, FAPESP and FUNDUNESP (Brazil); DAE and DST (India); Colciencias (Colombia); CONACyT (Mexico); KRF (Korea); CONICET and UBACyT (Argentina); FOM (The Netherlands); PPARC (United Kingdom); MSMT (Czech Republic); CRC Program, CFI, NSERC and WestGrid Project (Canada); BMBF and DFG (Germany); SFI (Ireland); Research Corporation, Alexander von Humboldt Foundation, and the Marie Curie Program.

[1] S. Eidelman et al, Phys. Lett. **B592**, 1 (2004)
[2] This limit is derived by combining limits from 13 different searches. Global fits to the CKM unitarity triangle are described in M. Battaglia *et al.*, "The CKM matrix and the unitarity triangle," arXiv:hep-ph/0304132, Oct. 2003.
[3] S. Catani, Yu.L. Dokshitzer, M. Olsson, G. Turnock, B.R. Webber, Phys.Lett. **B269** (1991) 432.
[4] T. Sjöstrand et. al. hep-ph/0108264
[5] DELPHI Collab., *b-tagging in DELPHI at LEP*, Eur. Phys. J. **C32** (2004), 185-208
[6] G. Borissov et al., *D0 Note 4875*, "Combined Opposite-side Flavor Tagging".
[7] Dzero collaboration, Phys. Rev. Lett. 94, 182001 (2005).
[8] H.G. Moser, A. Roussarie, Nucl.Instrum.Meth.A384:491–505, 1997.
[9] D.J. Lange, Nucl.Instrum.Meth.A462:152, 2001; for details see *http://www.slac.stanford.edu/~ lange/EvtGen.*
[10] G. Borisov and C. Mariotti, Nucl.Instrum.Meth.A372:181–187, 1996.
[11] B. Abbott et al., *D0 Note 4878*, "Search for B_s oscillations at D0 using $B_s \to D_s\mu X$ ($D_s \to K^*K$) decays".
[12] Heavy Flavor Averaging Group, arXiv:hep-ex/0505100.

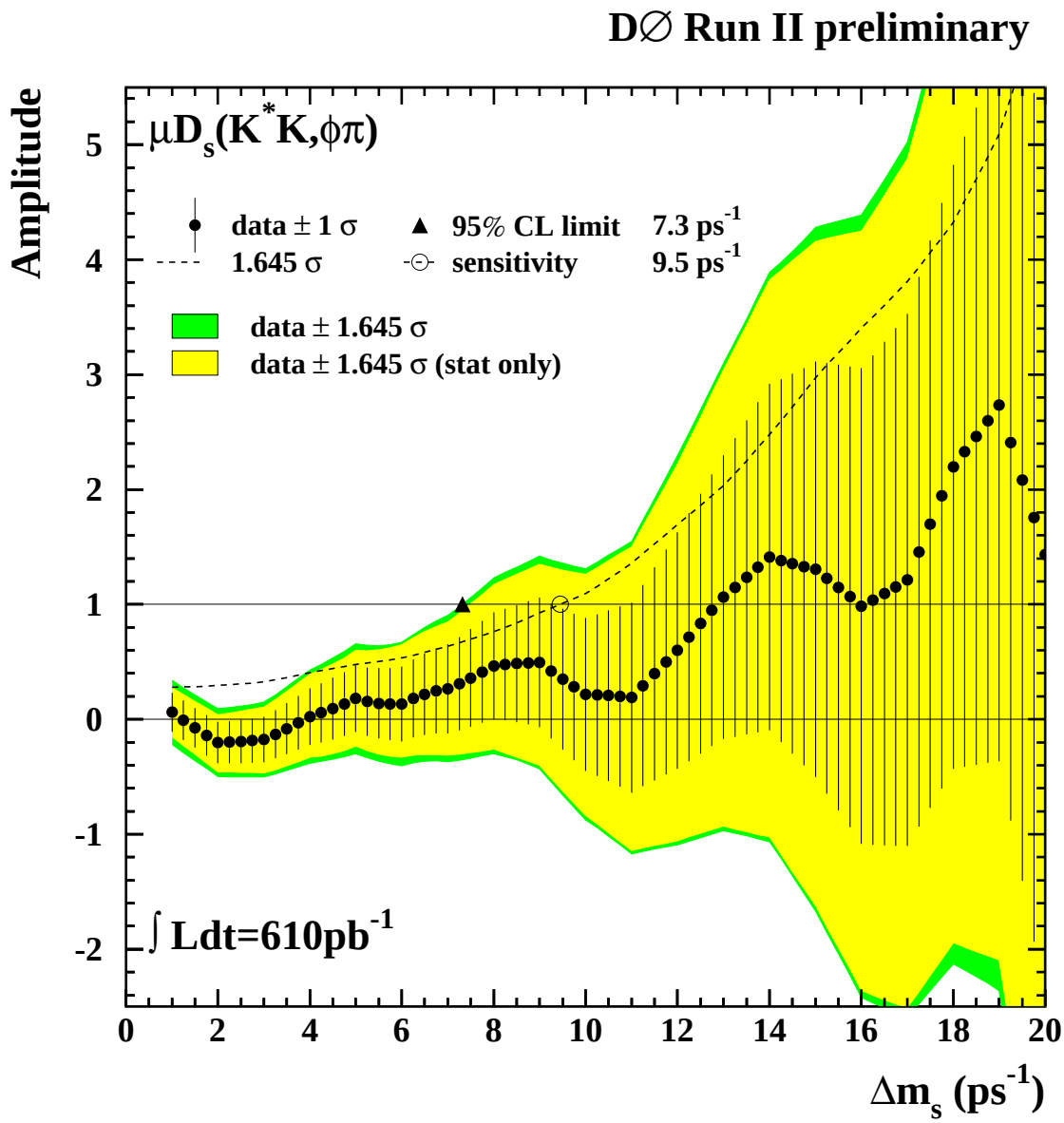

FIG. 11: Combined B_s^0 oscillation amplitude.